

Exciton fine structure in undoped GaN epitaxial films

D. Volm, K. Oettinger, T. Streibl, D. Kovalev, M. Ben-Chorin, J. Diener, and B. K. Meyer
Physics Department E16, Technical University of Munich, D-85747 Garching, Germany

J. Majewski
Walter-Schottky-Institute, Technical University of Munich, D-85747 Garching, Germany

L. Eckey and A. Hoffmann
Technical University Berlin, Institute for Solid-State Physics, Hardenbergstrasse 36, D-10623 Berlin, Germany

H. Amano and I. Akasaki
Department of Electrical and Electronic Engineering, Meijo University, 1-501 Shiogamaguchi, Tempaku-ku, Nagoya 468, Japan

K. Hiramatsu and T. Detchprohm
Department of Electronics, School of Engineering, Nagoya University, Furocho, Chikusa-ku, Nagoya 468-01, Japan
 (Received 27 November 1995)

We report on photoluminescence experiments on hexagonal GaN epitaxial films grown by hydride and organometallic vapor phase epitaxy on sapphire and 6H-SiC. At low temperatures we observe free and bound exciton recombinations, which allow us to establish the free-exciton binding energy and the localization energies of the excitons bound to neutral donors in undoped films. We demonstrate that the energetic positions of the excitonic recombination lines depend on the layer thickness and the substrate materials on which the layer was deposited. The influence of strain on the valence-band splittings can be quantified when observing the free-exciton transitions onto the different valence bands. The experimental results are compared to a theoretical calculation using a first-principle total-energy pseudopotential method within the local-density formalism. We present evidence for the existence of two shallow donors in GaN. One of them most likely stems from an intrinsic defect. [S0163-1829(96)05223-X]

I. INTRODUCTION

Since the first publication of Dingle *et al.*¹ on the excitonic and impurity related recombination in GaN epitaxial films, numerous investigations have focused on the luminescing properties of this material without being able to present a consistent picture. Excitonic recombination in GaN is a well-established fact, however, the scattering of energy positions is considerable.² An atlas of luminescence lines was compiled by Choyke,³ but he could not make a critical comment as to the results of the published works. Even for very high free carrier densities (as grown films are usually *n*-type conductive), excitonic emission dominates and is believed to stem from the annihilation of excitons at neutral shallow donors. In most cases, free-exciton emission was not observed. When growing GaN on sapphire or 6H-SiC substrates, the existing very large mismatch relaxes during the growth, by generating dislocations. Additionally, there is a thermal mismatch between substrate and layer caused by the different thermal expansion coefficients. Therefore, the excitonic line positions depend substantially on the layer thickness, i.e., strain decreases significantly with increasing thickness.⁴⁻⁶ The energy separation between the heavy, light, and spin-orbit-split hole valence bands is very sensitive to strain, too.

GaN with a wurtzite crystal structure is a direct band-gap semiconductor. The lowest fundamental gap is located at the Γ point. Due to the wurtzite crystal structure, the degeneracy

of the heavy and light hole valence bands does not apply any more and the bands are split apart by the crystal-field interaction. There is a general consensus on the fact that the Γ_{9V} band is located on top of the valence band giving rise to the FX(A) exciton observed in photoluminescence (PL) as the free exciton. The FX(B) and FX(C) excitons arising from lower Γ_{7V} and spin orbit split-off Γ_{9V} valence-band states have rarely been observed in PL so far, but were detected by absorption, PL-excitation (PLE) (Ref. 7), and reflexion measurements.¹ The valence-band parameters, i.e., the crystal-field splitting and the spin-orbit coupling constants in strain-free samples can be derived from the energetic positions of the excitons.

GaN epitaxial films are usually grown by organometallic vapor phase epitaxy (OMVPE) or by molecular beam epitaxy (MBE). OMVPE samples usually have an exciton linewidth between 3–4 meV. For MBE-grown layers linewidths above 10 meV are reported, thus making it impossible to resolve donor-bound excitons (D^0X) and free excitons (FX), in contrast to epitaxial films grown by the hydride vapor phase epitaxy (HVPE), where the neutral-donor-bound-exciton linewidth was as narrow as 1.4 meV.⁴ Free-exciton emission could also be observed. A similar sample was recently used in Zeeman experiments, there the D^0X linewidth was 1.2 meV at 4.2 K (Ref. 8).

The further improvement of OMVPE epitaxial growth using low temperature deposited buffer layers on sapphire and 6H-SiC substrates, now makes it possible to observe free and

bound excitons simultaneously in PL at low temperatures. Thus, we are able to study the influence of strain on the exciton line positions (Sec. III) for layers deposited on sapphire and on 6H-SiC. The observation of free-exciton recombination to the *B*- and *C*-valence bands allows us to quantify the strain-induced valence-band shifts (Sec. IV). The experimental values are compared with a theoretical analysis in Sec. V. In Sec. VI, we present a detailed spectroscopic study of the neutral-donor bound exciton using temperature dependent PL and PL under applied electrical field. We discuss our results in Sec. VII and end with a conclusion (Sec. VIII).

II. EXPERIMENTAL DETAILS

The HVPE sample No. 1 with a GaN layer thickness of 400 μm was grown without a buffer layer on *c*-plane sapphire. Details of the growth can be found in Ref. 4. The OMVPE GaN layers (sample No. 2 and No. 4) of 3 μm thickness were deposited on AlN buffers, either on *c*-plane sapphire or on 6H-SiC. The photoluminescence was excited with the 325 nm line of a HeCd laser. The emission was dispersed by a 1 m double monochromator (Jarrell Ash), the *f* number of which is 8 and detected by standard lock-in technique. The spectral resolution was higher than 0.5 meV at energies around 3.5 eV. The samples were placed in a temperature variable cryostat spanning the range from 1.5 to 300 K.

For the electric field dependent PL experiments, four contacts were soldered onto the sample using a Ga/In eutecticum. Current-voltage (*I-V*) measurements exhibited a good Ohmic behavior. Electric fields up to 14 V/cm were applied using a pulse generator and care was taken not to heat up the sample by varying the duty cycle. Rise and decay times of the optical response on the applied electric field did not exceed 20 ns. For the electrical PL measurements, the sample temperature was held constant at 1.5 K.

The details of the calorimetric measurements can be found in Ref. 9. Here, we give only a short description. Any absorption of radiation followed by nonradiative transitions increase the temperature of the excited medium. The measurement of the sample temperature as a function of the excitation wavelength is known as calorimetric absorption spectroscopy, and its sensitivity increases with decreasing temperature. Decreasing the temperature down to the mK range by using a $^3\text{He}/^4\text{He}$ dilution refrigerator leads to an extreme sensitivity of the set up. More details about the set up and its detection limit can be found in Ref. 9 and references therein.

III. THE FREE AND NEUTRAL-DONOR-BOUND-EXCITON LINE POSITION: EXPERIMENTAL RESULTS

Amano *et al.*⁵ and Naniwae *et al.*⁴ issued a detailed study of the influence of the layer thickness and strain on the c_0 - and a_0 -lattice constants and on the energy positions of the neutral-donor bound excitons. There is a significant lattice mismatch between GaN and sapphire or GaN and 6H-SiC, and there is also a difference in the thermal expansion coefficients of the materials. Amano *et al.* concluded that by growing on *c*-plane sapphire, the films are biaxially compressed (tensile for 6H-SiC) originating from first, the coher-

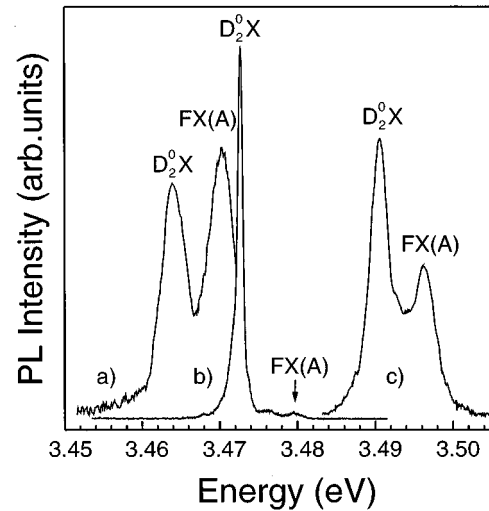


FIG. 1. Photoluminescence spectra of undoped GaN layers grown by OMVPE on 6H-SiC (a) on sapphire (c) and by HVPE on sapphire substrates (b). Free-exciton emission with the A-valence band [FX(A)] and neutral-donor-bound-exciton (D_2^0X) are observed ($T=1.5$ K).

ent growth and second, the difference in thermal expansion coefficients. The strain which is due to the lattice mismatch is relieved by the generation of misfit dislocations. The maximum shift of the D_2^0X line of 16 meV is explained by a lattice strain of 0.18% (strain parallel to the *c* axis). A layer of thickness 400 μm is assumed to be strain free.⁴⁻⁶

In Fig. 1, we compare the luminescence in the excitonic region for the HVPE (No. 1) and OMVPE layers (No. 2) grown on sapphire and on 6H-SiC (No. 4). In the OMVPE films, D_2^0X and free-exciton emission appears in comparable strength, for the HVPE film the free-exciton line is weaker, but completely resolved (linewidth is smaller by a factor of 2). The energetic positions are listed in Table I. The 400 μm thick layer represents the strain-free case. For 3 μm thin films, there is an apparent blueshift or redshift depending on whether sapphire or 6H-SiC is used as a substrate material. In Fig. 2, we collect the results. For comparison, we include the corresponding values of a 50 μm HVPE GaN layer on sapphire⁴ and of a 80 μm thick GaN layer on 6H-SiC, grown by the sublimation sandwich technique.¹⁰ Under biaxial compression (sapphire substrate), the blueshift of the FX(A) exciton amounts to ≈ 17 meV, whereas under biaxial tension (6H-SiC substrate) the redshift is ≈ 10 meV. One also notes that the energetic distance between the free and the neutral-donor-bound exciton (D_2^0X) increases from 6.2 meV to 7.2 meV from thin to thick films.

IV. THE FREE-EXCITON TRANSITIONS

Tensile and compressive strains also modify the valence-band splittings. It was therefore our aim, using different spectroscopic techniques, to resolve and identify free-exciton transitions onto the different valence-band states. The free-exciton transitions to the *B*- and *C*-valence bands in hexagonal compound semiconductors are usually observed using photoluminescence excitation or in reflection. Here, we applied calorimetric spectroscopy in the mK range. Figure 3

TABLE I. Energetic positions of the various free and bound exciton lines in GaN on Al₂O₃ and 6H-SiC epitaxial layer. Temperature was in all cases 1.5 K, the accuracy is better than ± 0.5 meV. The values for sample No. 3 were taken from Ref. 4, for sample No. 5 from Ref. 10.

Samples	Substrate	Thickness in μm	FX(C)	FX(B)	FX(A) $n=2$	FX(A) $n=1$	D_1^0X	D_2^0X	D_2^+X
No. 1	Al ₂ O ₃	400	3.5025	3.4860	3.4995	3.4799	3.4762	3.4727	
No. 2	Al ₂ O ₃	3		3.5050	3.5162	3.4962	3.4935	3.4900	3.4865
No. 3	Al ₂ O ₃	50				3.483		3.477	
No. 4	6H-SiC	3			3.4905	3.4703		3.4639	
No. 5	6H-SiC	80				3.4795		3.4723	

shows highly resolved calorimetric absorption (CAS), calorimetric transmission (CTS), and calorimetric reflection (CRS) of a 400 μm GaN/Al₂O₃ epilayer. Three structures are clearly resolved in the CRS spectrum and attributed to the excitons FX(A) at 3.4799 eV, FX(B) at 3.486 eV, and FX(C) at 3.5025 eV, involving holes from the A-, B-, and C-valence bands, respectively. The differences of energies of these values represent the splitting of the three valence bands of a strain-free GaN epilayer. A minor structure is detected at 3.4995 eV and ascribed to the FX(A) $n=2$ exciton. Thus, the value of 26.1 meV for the free-exciton binding energy can be calculated (see below). Since a reduction of the reflectivity implies an increase of light absorption in the crystal, which in turn triggers nonradiative processes, the same structures as in CRS are also seen in the CAS. An additional structure in the CAS appears as a dip at 3.4727 eV. It is caused by the neutral-donor-bound-exciton absorption in transmission (the transmission coefficient is nearly zero in this range). Thus, the calorimetric detection of the donor-bound-exciton absorption demonstrates the advantage and high sensitivity of the CAS technique. The decrease of the CAS signal at the spectral position of the D^0X line implies a decrease of the phonon emission rate and, therefore, an enhanced radiative relaxation. The addition of the CTS, CRS, and CAS shows that in this sample the quantum efficiencies of the donor-bound exciton and of the free exciton are 50% and 25%, respectively. In the inset of Fig. 3, the reflectivity loop of the FX(A) is fitted by a polariton model.¹¹ From the best fit, we obtain the following parameters: The eigenfre-

quency ω_0 of the FX(A) is 3.480 eV, and the damping constant Γ , which is a direct measure of the polariton-impurity interaction, is 0.65 meV, showing that the quality of the epilayer is relatively good. The longitudinal-transversal splitting of the exciton ω_{LT} , which is proportional to the oscillator strength of the exciton, is 0.64 meV. The background dielectric constant ϵ_0 is 9.7, and the perpendicular components of the effective masses of the hole and the electron are $0.75m_0$ and $0.23m_0$, respectively.

The free-exciton transitions into the A-, B-, and C-valence bands could also be observed by PL for the 400 μm thick layer. In Fig. 4, we show the details of PL above the D^0X line on an expanded logarithmic scale. The transition energies to the B- and C-valence bands (marked in Fig. 3 with B and C) are in perfect agreement with the CAS results. We identify an additional line as being the FX(A) $n=2$ transition. The FX(B) and FX(A) $n=2$ transitions [see Fig. 4(c)] are also seen in the OMVPE layer (see also Table I). The FX(A) $n=2$ transition, i.e., the exciton in the first excited Rydberg state, is 20 ± 0.5 meV above the ground state. This is 3/4 of the binding energy in the effective-mass approximation. The free-exciton binding energy is hence calculated to be 26.7 ± 0.5 meV. For GaN on 6H-SiC the FX(A) $n=2$ and FX(B) were not observable in PL, how-

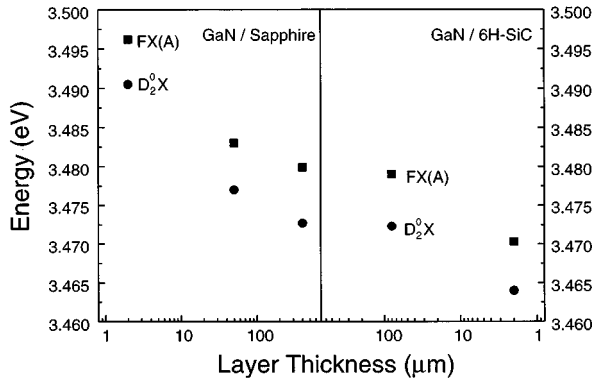


FIG. 2. Energetic positions of the center of gravity of the neutral-donor-bound and free exciton as a function of layer thickness for GaN layer deposited on sapphire and 6H-SiC substrates.

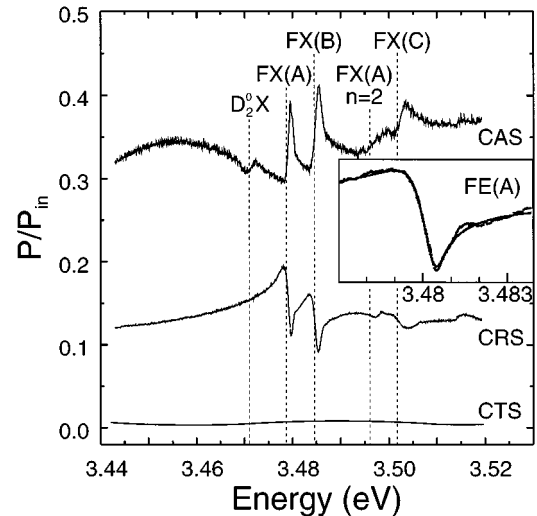


FIG. 3. Calorimetric absorption (CAS), reflection (CRS), and transmission (CTS) spectra of the 400 μm thick HVPE GaN/sapphire layer ($T = 45$ mK). In the inset, a fit to the reflection spectrum of the FE(A) exciton is shown (for details see text).

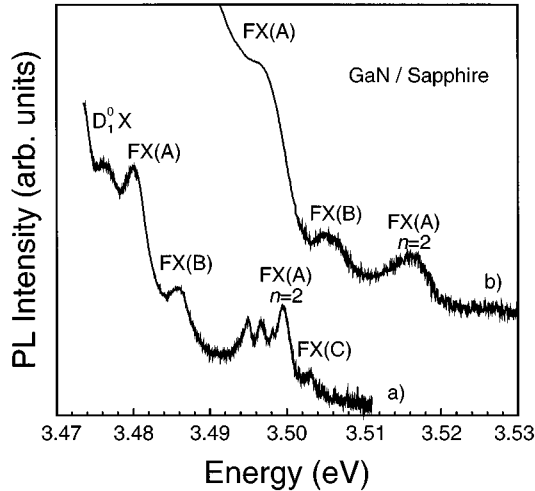


FIG. 4. High spectral resolution photoluminescence in the energetic region above the neutral-donor-bound exciton line. Transitions to the lower B - and C -valence bands are indicated. The $n=2$ excited state transition of the A exciton is also seen. (a) HVPE film; (b) OMVPE layer ($T=1.5$ K).

ever, the $\text{FX}(A)$ $n=2$ transition was seen in PLE. The free-exciton binding energy coincides with GaN on sapphire. The identification of the free-exciton transition is primarily, but not only based on the comparison with reflectivity measurements (see above). We also carefully studied the temperature dependence of the luminescence lines and deduced an activation energy for the A exciton (26 ± 1 meV), which is in agreement with the experimental results, which stipulate that the $\text{FX}(A)$ $n=2$ state is 20 meV above the found ground state. Moreover, with an increase in temperature, the characteristic Maxwell-line shapes develop for all free-exciton lines. Further details together with results from luminescence excitation measurements will be reported in Ref. 12.

V. THEORETICAL CALCULATION OF THE STRAIN-INDUCED SHIFT OF THE VALENCE BANDS AND COMPARISON WITH EXPERIMENT

We treat the strain-induced shift of the three valence bands with respect to the conduction band as follows. Our calculations are based on the first-principles total-energy pseudopotential method within the local-density-functional formalism.¹³ We used norm-conserving separable pseudopotentials¹⁴ and a preconditioned conjugate gradient algorithm¹⁵ for minimizing the total crystal energy, with respect to electronic as well as ionic degrees of freedom. These pseudopotentials guarantee that the kinetic energy cutoff at 62 Ry, used in this calculation, gives very good convergence of the total energy. The set of 14 special points¹⁶ is used to perform k -space integrations. The semicore Ga $3d$ electrons are treated as part of the frozen core, but their considerable overlap with the valence electrons is accounted for by including the nonlinear core exchange-correlation correction.¹⁷ This procedure increases the transferability of the pseudopotentials and yields lattice constants that agree very well with experiment. The computed lattice constants for GaN in the wurtzite phase are $a_0=3.174$ Å (3.189 Å) (Ref. 18), $c_0=5.169$ Å (5.185 Å) (Ref. 18), $u=0.377$ (0.377) (Ref. 19),

$c_0/a_0=1.628$ (1.626), with the experimental values given in parentheses. The calculations for the biaxially strained crystal in the (0001) plane were carried out as follows. For a given lattice constant a corresponding to the in-plane strain $\epsilon_{\parallel}=(a-a_0)/a_0$, we obtained the values of c and u by the total-energy minimization method. Then, the band structure was computed for the optimized geometry. The spin-orbit interactions were taken into account nonperturbatively through the relativistic pseudopotentials. The details of these calculations will be published elsewhere.²⁰ Here, we focus on the energy gap and on the valence-band maximum at the Γ point. In the absence of the spin-orbit interaction, the top of the valence band is split into twofold- and single-degenerated states, Γ_6 and Γ_1 , respectively. The arrangement of these levels depends on the biaxial strain in the system. We found out that for compressive as well as for tensile biaxial strain up to 0.25%, the Γ_6 lies above the Γ_1 . For larger tensile strains ($\epsilon_{\parallel}>0.25\%$), the order of these levels is reversed with the Γ_1 state lying higher. The energy splitting between these two levels is induced by the hexagonal symmetry of the wurtzite structure, this is why it is called the crystal-field splitting Δ_{cr} , ($\Delta_{\text{cr}}=\epsilon_{\Gamma_6}-\epsilon_{\Gamma_1}$). The strain dependence of the Δ_{cr} for ϵ_{\parallel} between -2% and 2% can be described by the relation $\Delta_{\text{cr}}(\epsilon_{\parallel})\approx\Delta_{\text{cr}}(0)+\alpha_{\Delta}\epsilon_{\parallel}$, where the crystal-field splitting $\Delta_{\text{cr}}(0)$ without strain is 0.035 eV, and the linear coefficient α_{Δ} is -9 eV. The spin-orbit interaction splits the twofold-degenerated state Γ_6 , in such a manner that the top of the valence band consists of three levels with energies ϵ_C , ϵ_B , ϵ_A , with $\epsilon_A>\epsilon_B>\epsilon_C$. The energy gaps between these levels and the conduction-band bottom ϵ_{cbb} , namely $E_I=\epsilon_{\text{cbb}}-\epsilon_I$, with ($I=A,B,C$), as a function of the biaxial strain ϵ_{\parallel} , are depicted in Fig. 5. In the case of unstrained GaN, we obtain $\epsilon_{BA}=\epsilon_B-\epsilon_A=-0.008$ eV, and $\epsilon_{CA}=\epsilon_C-\epsilon_A=-0.043$ eV for the valence-band splittings. The computed values of ϵ_{BA} and ϵ_{CA} agree fairly well with our experimental values, namely $\epsilon_{BA}=-0.006$ (-0.006 eV),²¹ and $\epsilon_{CA}=-0.022$ eV (-0.018 eV, -0.027 eV) (Ref. 21), with experimental values taken from the literature given in parenthesis. Without strain, the analytical solutions of the effective mass Hamiltonian at the Γ point²² give the following energy levels:

$$E_1=\Delta_{\text{cr}}+\Delta_2, \quad (1)$$

$$E_{2,3}=\frac{\Delta_{\text{cr}}-\Delta_2\pm\sqrt{(\Delta_{\text{cr}}-\Delta_2)^2+8\Delta_3^2}}{2}, \quad (2)$$

where Δ_2 and Δ_3 are spin-orbit coupling constants. Using computed values of the splittings ϵ_{BA} and ϵ_{CA} and crystal-field splitting parameter Δ_{cr} from the calculation without the spin-orbit interaction, we have found Δ_2 and Δ_3 to be equal 0.005 eV and 0.007 eV, respectively. For low biaxial strain (between -1% and 1%), the changes of the fundamental energy gap with the strain ϵ_{\parallel} can be described by the following relation, $E_{\text{gap}}(\epsilon_{\parallel})=E_{\text{gap}}(0)+b\epsilon_{\parallel}$. The value of the coefficient b obtained from the theoretical calculations is equal to -5.5 eV for $\epsilon_{\parallel}<0.25\%$, and -13 eV for $\epsilon_{\parallel}>0.25\%$. This change of the slope is connected to the crossing of the Γ_6 and Γ_1 levels with tensile strain, as discussed above. On the basis of our experiments for compressive strain, we established the value of b to be -8.2 eV for the compressive

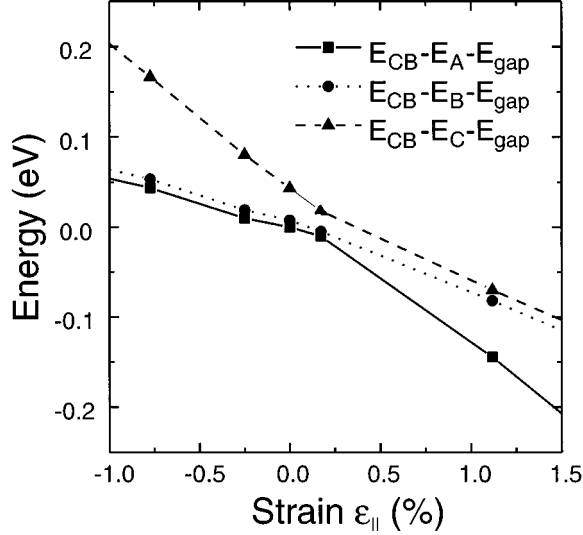


FIG. 5. Energy shifts of the A-, B- and C-valence band as a function of strain as calculated theoretically (for details see text).

strain region and -13 eV for the tensile strain region. The agreement with the theoretical value is good taking into account that, first, in the experiment the values of the strain were not measured directly, but estimated from the thermal expansion coefficients, second, that we performed standard local-density approximation calculations and that there even the small changes of the self-energies with strain can have an impact.²³ The deformation potential b for the biaxial strain is much smaller than the computed deformation potential for the hydrostatic pressure $a_h = \Delta E_{\text{gap}}/\epsilon_{||} = -24.7$ eV [it corresponds to $a = \Delta E_{\text{gap}}/(\Delta V/V) = -8$ eV, where $\Delta V/V = 2\epsilon_{||} + \epsilon_{\perp}$]. It is connected to the fact that the strain in the (0001) direction ϵ_{\perp} obtained from the minimization of the total energy has always the same sign as the in-plane strain $\epsilon_{||}$ for the hydrostatic pressure, whereas in the case of biaxial strain ϵ_{\perp} and $\epsilon_{||}$ differ in sign.

In order to calculate the thermally induced strain, we assume that at growth temperature the epitaxial layer is relaxed, i.e., $a_{\text{epi}} = a_{\text{sub}} = a_0$. We consider only the linear thermal expansion coefficients²¹ $\alpha_{\text{GaN}} = 5.59 \times 10^{-6}$ 1/K, $\alpha_{6H\text{-SiC}} = 4.8 \times 10^{-6}$ 1/K, and $\alpha_{\text{sapphire}} = 7.5 \times 10^{-6}$ 1/K in the equation $a = a_0(1 + \alpha\Delta T)$. Using $\epsilon_{xx} = (a_{\text{sub}} - a_{\text{epi}})/a_{\text{sub}}$, we obtain for a temperature difference of $\Delta T = 1000$ K,

$$\epsilon_{xx} = \frac{(\alpha_{\text{sub}} - \alpha_{\text{GaN}})\Delta T}{1 + \alpha_{\text{sub}}\Delta T} \approx (\alpha_{\text{sub}} - \alpha_{\text{GaN}})\Delta T, \quad (3)$$

TABLE II. The binding and localization energies of the various recombination centers together with the corresponding dissociation processes for GaN on Al_2O_3 with $3 \mu\text{m}$ thickness.

Recombination center	Binding / Localization energy in meV	Transition energy	Dissociation process
FX	26.7 ± 0.5	$E_g - E_{\text{FX}}$	$\text{FX} \rightarrow e + h$
$D_1^0 X$	2.7 ± 0.5	$E_g - (E_{\text{FX}} + \alpha E_{D1})$	$D_1^0 X \rightarrow D_1^0 + \text{FX}$
$D_2^0 X$	6.2 ± 0.5	$E_g - (E_{\text{FX}} + \alpha E_{D2})$	$D_2^0 X \rightarrow D_2^0 + \text{FX}$
$D_2^+ X$	6.2 ± 0.5	$E_g - (E_{D2} + \alpha E_{D2})$	$D_2^+ X \rightarrow D_2^+ + \text{FX}$

which yields for GaN on sapphire $\epsilon_{||} = 0.2\%$ and for GaN on 6H-SiC $\epsilon_{||} = 0.07\%$.

VI. DONOR-BOUND EXCITONS

The nature of the defects causing n -type conductivity in undoped GaN epitaxial films is still not sure yet. Following recent theoretical arguments, native defects as well as extrinsic impurities are believed to be responsible.^{24–27} The nitrogen vacancies or the gallium interstitials are the prime candidates for intrinsic defects, they should induce a shallow effective-mass-type state in GaN. The extrinsic defects introducing shallow donor levels could come from the group VI elements on group V site. Oxygen would be one candidate. From the group IV elements, the Si on Ga site is a very efficient donor dopant.

The neutral-donor-bound exciton recombination is 6–7 meV lower in energy compared to the FX(A) transition (see Fig. 2 and Table I). It is its localization energy (see Table II), and in many semiconductors there is a well-defined proportionality to the respective donor binding energy ($E_L = \alpha E_D$) named Haynes rule.²⁸ Based on our measurements of the electron cyclotron resonance in OMVPE GaN (Ref. 29), which gave a mass of $m^* = 0.22m_0$ (polaron mass), an estimation of the binding energy of the effective-mass type donor was possible. Using a static dielectric constant of $\epsilon = 9.7$, one obtains $E_D = 31.7 \pm 1$ meV.

It comes as a surprise that under high spectral resolution, the donor-bound exciton line was not a single line; clearly two transitions can be seen, separated by approximately 3 meV. This observation is not specific to the OMVPE layers, but occurs also in the $400 \mu\text{m}$ thick HVPE films. The transitions could arise from two independent donor-bound exciton lines, this means that also two shallow donors should exist in GaN. It is also possible that the excited states of either the donor or the exciton are observed. The observation of the excited state of the donor is less likely because the energy separation should be 3/4 of the effective Rydberg, i.e., 3/4 of 31.7 meV. An excited state of the neutral-donor-bound exciton may account for the high energy line. The possibility that they arise from donor-bound excitons involving the A- and B-valence bands can be ruled out, since the energetic distance between A and B bands is ≈ 9 meV for sample No. 2. It was, therefore, our interest to gain more spectroscopic information for which PL measurements under applied electrical field were performed. Free electrons are created under band to band excitation; they can be accelerated in the electrical field within the contact distance. The gain in energy in the electrical field is used to impact ionize

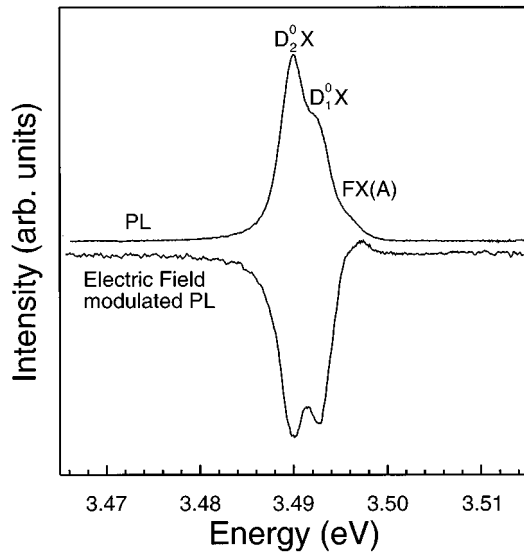


FIG. 6. High-resolution photoluminescence (a) of a OMVPE GaN layer on sapphire. The free-exciton line and two neutral-donor-bound-exciton lines are resolved. They are seen in electrical field modulated luminescence as a decrease and an increase, respectively ($T=1.5$ K).

free or bound excitons or neutral donors. If the free-exciton binding energy is high compared to the localization energy of excitons at the impurities, the impact ionization will create free excitons, dissociating bound excitons. The absence of deviation of the I - V curve from linear regime under impact ionization suggests that bound exciton states are dissociated into the free exciton and neutral-donor states. This is observed in the experiment. In Fig. 6, we compare the PL spectrum of sample No. 2 with the optically detected impact ionization (ODII) spectrum (changes of PL under electrical field synchronously detected). In the ODII spectrum the free exciton appears as an increase, the donor-bound exciton transitions are quenched by the electrical field and are hence seen as a decrease. In Fig. 7, we show the evolution of the two

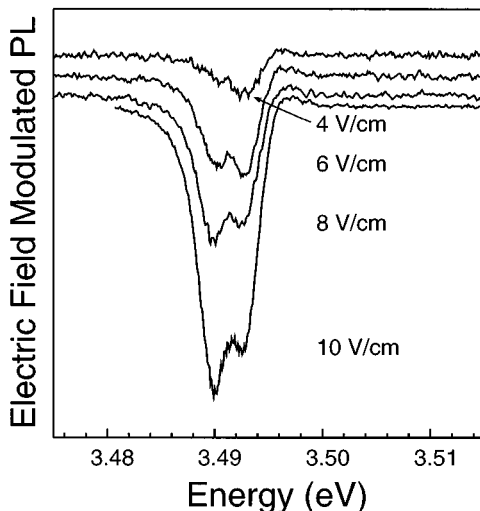


FIG. 7. Electrical field-modulated photoluminescence for different fields applied ($T=1.5$ K).

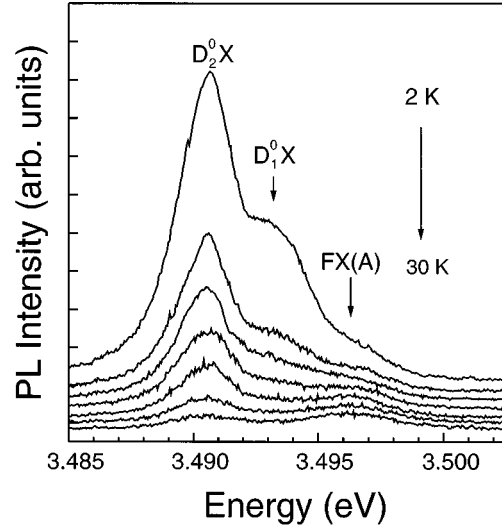


FIG. 8. Temperature-dependent photoluminescence measurements which show two neutral-donor-bound exciton transitions and the free-exciton line (OMVPE GaN on sapphire).

transitions in the donor-bound exciton range for different voltages. At low fields, the high energy transition becomes stronger, at 6 V/cm both transitions have equal intensities and at fields of 12 V/cm the line at the lower energy is strongest. This provides the first evidence for two individual donor-bound excitons. The one with the smaller localization energy (high energy line) will be ionized, due to the impact process at lower fields. In order to confirm the results, we studied the PL in the temperature range between 1.5 K and 20 K (Fig. 8). In the temperature dependent measurements, the decrease in line intensity (the thermal activation energy) is again a measure of the localization energy. It comes as no surprise that the high energy transition decreases more rapidly in intensity; at 20 K only the low energy transition and the free exciton can be seen. If we assume that both lines are caused by exciton excited states, thermalization should result in equal intensities at higher temperatures. Based on these observations, we can now accurately determine the localization energies, the energetic distances to the free exciton. We obtain (2.7 ± 0.1) meV and (6.2 ± 0.1) meV and label them D_1^0X and D_2^0X , respectively. At energies below the donor-bound excitons, i.e., at 3.4865 eV for the OMVPE sample on sapphire, an additional transition was seen. It is (9.7 ± 0.5) meV below the free-exciton FX(A) transition, and attributed as outlined below to the exciton bound to an ionized donor (D_2^+).

VII. DISCUSSION

The past four years have brought a tremendous breakthrough in the quality of GaN epitaxial films. The free carrier concentration in undoped films now reaches values around $5 \times 10^{16} \text{ cm}^{-3}$ and less, and mobilities at helium temperatures of $4000 \text{ cm}^2/(\text{V s})$ are achievable.²⁹ The optical properties were improved considerably as well, allowing for the observation of free-exciton excited states for the first time. The information obtained can now be used to quantify and verify important parameters of the semiconductor GaN, such

as free-exciton binding energies, localization energies of excitons bound to impurities, electron and hole effective masses. It is also possible to see that the n -type conductivity might not be linked to one “omnipresent” residual donor only. The scatter in the data, with respect to energetic positions of excitons, is now understood and ascribed to the influence of strain (layer thickness).

The observation of free-exciton recombination involving the B - and C -valence bands offered the possibility to quantify the influence of strain caused by the difference in thermal expansion coefficients of GaN and the sapphire substrate. In the relaxed films from the energetic distance, the value for the crystal field and spin-orbit splitting could be calculated.¹ One obtain $\Delta = 11$ meV for the crystal field and for $\lambda = 17$ meV. In thin films, the splittings between A to B , and B to C bands are different. There is consistency between the absolute value of the strain using the line positions of the A and B excitons as done in this work and measurements of the change of the lattice constants in c and a direction as shown in Refs. 4–6. One may wonder why the recombination to the deeper valence bands can be observed at all. Usually the photogenerated holes relax very quickly (within picoseconds) to the top of the valence band, i.e., only the FX(A) exciton should luminesce. However, since the energetic distances between A - and B -, and A - and C -valence bands are much smaller than the optical phonon energy (the LO phonon energy is 92 meV), the relaxation of the photogenerated holes by optical phonon is inhibited. Relaxation can thus only proceed via acoustical phonons and obviously there is a bottleneck. The energy relaxation time due to acoustical phonons is much longer than due to optical ones and could be comparable to or even longer than the lifetimes of the B - and C -exciton states [the FX(A) exciton has a 20 ps decay time at 1.5 K (Ref. 30)]. Under such conditions, one could expect to detect the recombination from B - and C -exciton states. Time-resolved experiments are planned to further address this point.

Using the energetic position of the free A exciton and adding the free-exciton binding energy, we derive for the band-gap energies: 3.523 eV for $d \leq 3 \mu\text{m}$ thin films on sapphire, 3.506 eV for the strain-free sample and for the thin films ($d \leq 3 \mu\text{m}$) on 6H-SiC 3.497 eV.

In principle, the electron and hole masses can be calculated from the free-exciton binding energy. In hexagonal crystals with anisotropy of the dielectric constant and the effective electron and hole masses, this analysis is discussed in detail by Flohrer *et al.*:³¹ The corresponding effective Rydberg R_i is

$$R_i = \frac{e^4 \mu_i}{2 \hbar^2 \epsilon^2}, \quad (4)$$

where $\bar{\epsilon}$ is $\sqrt{\epsilon_{\parallel} \epsilon_{\perp}}$ and μ_i is related to the electron and hole masses by

$$\frac{1}{\mu_i} = \frac{2}{3} \frac{1}{m_i^{\perp}} + \frac{1}{3} \frac{\epsilon_{\perp}}{\epsilon_{\parallel} \mu_i^{\parallel}} = \frac{1}{m_e} + \frac{1}{\mu_i}, \quad i = A, B, \quad (5)$$

$$\frac{1}{m_i} = \frac{2}{3} \frac{1}{m_i^{\perp}} + \frac{1}{3} \frac{\epsilon_{\perp}}{\epsilon_{\parallel} m_i^{\parallel}}, \quad i = e, A, B. \quad (6)$$

$\mu_{A,B}^{\perp}$ and $\mu_{A,B}^{\parallel}$ are the reduced masses for the A and B excitons perpendicular and parallel to the c axis, respectively. Only the electron effective mass is known from the experiment, hence m_A^{\parallel} and m_A^{\perp} cannot be calculated from the exciton binding energy. From the CAS experiments, we obtained $m_{hh}^* = 0.75m_0$ and $m_e^* = 0.22m_0$ (polaron masses).

In earlier investigations on the properties of donor-bound excitons, localization energies between 6 and 7 meV and donor binding energies from 30 to 40 meV have been reported.² For the effective-mass value, we calculate 31.7 meV.

A single description of the localization energy of the impurity-bound excitons is usually looked for in terms of Hayne’s rule.²⁸ It means that for the localization energy of the exciton, with respect to the binding energy of the impurity (E_D for the donors, E_A for the acceptors), a constant ratio is found. In a semiempirical theory, Halsted and Aven³² derived for the ratios the following result $\alpha = E_L/E_D = 0.2$ and $\beta = E_L/E_A = 0.1$, in line with the work from Hopfield.³³ However, Hayne’s rule does not always apply. CdTe is an example where it holds for the donors ($\alpha = 0.245$), but for the neutral-acceptor-bound excitons β ranges between 0.05 and 0.13. We assume that D_2^0X with $E_L = 6.2$ meV is connected with the effective-mass-type donor of 31.7 meV and the proportionality constant is 0.195.

The value for the donor binding energy of 31.7 meV is also consistent with the recombination energy of the ionized-donor-bound exciton. As can be read from Table II its transition occurs at $E_g - (E_D + \alpha E_D)$ compared to the neutral-donor-bound exciton energy at $E_g - (E_{FX} + \alpha E_D)$. If we assume that the localization energy (αE_D) is the same, the D^+X line is lower in energy by the difference between E_D and E_{FX} , in agreement with the experimental results.

One may wonder why in thick strain-free films the localization energy amounts to 7.2 meV instead of 6.2 meV. We noticed a small difference in the free-exciton binding energies (26.1 meV to 26.7 meV), which obviously reflects the modification of the valence-band structure under strain (change in hole masses) and the difference of 1 meV can probably be attributed to strain effects.

A point we want to discuss further is the neutral-donor-bound exciton which has a localization energy of 3.7 meV in sample No. 1 and 2.7 meV in sample No. 2. Assuming that Hayne’s rule holds results in a corresponding donor binding energy of 19 meV and 14 meV, respectively. It would mean that instead of a negative central cell shift (deepening of the level, as it is usually the case, when going from a light element to the heavier element in the same row of the Periodic Table), one has a positive central cell shift.

A shallow state (localized in \vec{r} space) induced by the Coulomb potential of a deep resonance state in the conduction band could have a positive central cell shift. Thus, the D_1^0X line could arise from a donor which is of intrinsic origin, e.g., the N vacancy (V_N) or the Ga interstitial (Ga_i).^{24–27}

VIII. CONCLUSION

Free and impurity-bound exciton recombinations were studied in hexagonal undoped GaN films differing in layer thickness. Transition energies strongly depend on the sub-

strate materials used and on the layer thickness, which reflect the influence of the residual strain due to differences in thermal expansion coefficients between layers and substrates. We quantify this relation both experimentally and theoretically. The free-exciton binding energy as well as the energy gaps for thin and thick layers are obtained with very high accuracy. We demonstrate that two shallow donors are present in undoped films based on the observation of two neutral-donor-bound exciton lines. We speculate that V_N or

Ga_i and Si_{Ga} could be the source of n -type conductivity in undoped GaN films.

ACKNOWLEDGMENTS

We thank the D.F.G. for financial support and A.L. Efros for his comments on many details of the excitons in semiconductors. D. Kovalev acknowledges the support of the Alexander von Humboldt Foundation.

- ¹R. Dingle, D.D. Sell, S.E. Stokowski, and M. Illegems, *Phys. Rev. B* **4**, 1211 (1971).
- ²S. Strite and H. Morkoc, *J. Vac. Sci. Technol. B* **10**, 1237 (1992).
- ³W.J. Choyke and I. Linkov, in *Silicon Carbide and Related Materials*, edited by M. G. Spencer, R. P. Devaty, J. A. Edmond, M. Asif Khan, and M. Rahman, IOP Conf. Proc. No. 137 (Institute of Physics and Physical Society, London, 1994), p. 141.
- ⁴K. Naniwae, S. Itoh, H. Amano, K. Itoh, I.K. Hiramatsu, and I. Akasaki, *J. Cryst. Growth* **99**, 381 (1990).
- ⁵H. Amano, K. Hiramatsu, and I. Akasaki, *Jpn. J. Appl. Phys.* **27**, L1384 (1988).
- ⁶K. Hiramatsu, T. Detchprohm, and I. Akasaki, *Jpn. J. Appl. Phys.* **32**, 1528 (1993).
- ⁷B. Monemar, *Phys. Rev. B* **19**, 676 (1974).
- ⁸D. Volm, T. Streibl, B.K. Meyer, T. Detchprohm, H. Amano, and I. Akasaki, *Solid State Commun.* **96**, 53 (1995).
- ⁹L. Podlowski, A. Hoffmann, and I. Broser, *J. Cryst. Growth* **117**, 698 (1992).
- ¹⁰C. Wetzel, D. Volm, B.K. Meyer, K. Pressel, S. Nilsson, E.N. Mokhov, and P.G. Baranov, *Appl. Phys. Lett.* **65**, 1033 (1994).
- ¹¹I. Broser and M. Rosenzweig, *Phys. Rev. B* **22**, 2000 (1980).
- ¹²D. Kovalev, B. Averboukh, D. Volm, B.K. Meyer, H. Amano, and I. Akasaki (unpublished).
- ¹³W.E. Pickett, *Comput. Phys. Rep.* **9**, 115 (1989).
- ¹⁴N. Troullier and J.L. Martins, *Phys. Rev. B* **43**, 1993 (1991); L. Kleinman and D.M. Bylander, *Phys. Rev. Lett.* **48**, 1425 (1982).
- ¹⁵M.C. Payne, M.P. Teter, D.C. Allan, T.A. Arias, and J.D. Joannopoulos, *Rev. Mod. Phys.* **64**, 1045 (1992).
- ¹⁶P.J.H. Denteneer and W. Van Haeringen, *Solid State Commun.* **59**, 829 (1986).
- ¹⁷S.G. Louie, S. Froyen, and M.L. Cohen, *Phys. Rev. B* **26**, 1738 (1982).
- ¹⁸S. Strite, M.E. Lin, and H. Morkoc, *Thin Solid Films* **231**, 197 (1993).
- ¹⁹H. Schulz and K. Thiemann, *Solid State Commun.* **23**, 815 (1977).
- ²⁰J.A. Majewski and P. Vogl (unpublished).
- ²¹*Physics of Group IV Elements and III-V Compounds*, edited by K.-H. Hellwege, Landolt-Börnstein, New Series, Group III, Vol. 17, Pt. a (Springer, Berlin, 1982); *Intrinsic Properties of Group IV Elements and III-V, II-VI and I-VII Compounds*, edited by O. Madelung, M. Schulz, and H. Weiss, Landolt-Börnstein, New Series, Group III, Vol. 22, Pt. a (Springer, Berlin, 1982); *Electronic Structure of Solids*, edited by A. Goldman and E.-E. Koch, Landolt-Börnstein, New Series, Group II, Vol. 33, Pt. a (Springer, Berlin, 1989).
- ²²G.L. Bir and G.E. Pikus, *Symmetry and Strain-Induced Effects in Semiconductors* (Wiley, New York, 1974).
- ²³M. Palumbo, L. Reining, R.W. Godby, C.M. Bertoni, and N. Börnsen, *Europhys. Lett.* **26**, 607 (1994).
- ²⁴P. Boguslawski, E. Briggs, T.A. White, M.G. Wensell, and J. Bernholc, in *Diamond, SiC and Nitride Wide Bandgap Semiconductors*, edited by C.H. Carter, Jr., G. Gildenblat, S. Nakamura, and R.J. Nemanichi, MRS Symposia Proceedings No. 339 (Materials Research Society, Pittsburgh, 1994), p. 693.
- ²⁵P. Boguslawski, E. Briggs, and J. Bernholc, *Phys. Rev. B* **51**, 17 255 (1995).
- ²⁶J. Neugebauer and C.G. Van de Walle, *Phys. Rev. B* **50**, 8067 (1994).
- ²⁷T.L. Tansley and R.J. Eagan, *Phys. Rev. B* **45**, 10 942 (1992), and references therein.
- ²⁸J. R. Haynes, *Phys. Rev. Lett.* **4**, 351 (1960).
- ²⁹M. Drechsler, B.K. Meyer, D. Detchprohm, H. Amano, and I. Akasaki, *Jpn. J. Appl. Phys.* **34**, L1178 (1995).
- ³⁰L. Eckey, R. Heitz, A. Hofmann, I. Broser, B.K. Meyer, T. Detchprohm, H. Amano, and I. Akasaki (unpublished).
- ³¹J. Flohrer, E. Jahne, and M. Porsch, *Phys. Status Solidi* **91**, 467 (1979).
- ³²R.E. Halsted and M. Aven, *Phys. Rev. Lett.* **14**, 64 (1965).
- ³³J.J. Hopfield, *J. Phys. Chem. Solids* **15**, 97 (1960).